JHEP PROCEEDINGS

International Europhysics Conference on HEP

Total Cross Section in $\gamma\gamma$ Collisions at LEP

Luca Malgeri*

DPNC - University of Geneva - 24, quai E. Ansermet 1211 Genève 4 (Switzerland)
E-mail: Luca.Malgeri@cern.ch

Abstract: The reaction $e^+e^- \to e^+e^-\gamma^*\gamma^* \to e^+e^-$ *hadrons* for quasi-real photons is studied at LEP using data from $\sqrt{s} = 130$ GeV up to 202 GeV. Results on the total cross sections $\sigma(e^+e^- \to e^+e^-$ *hadrons*$)$ and $\sigma(\gamma\gamma \to$ *hadrons*$)$ are obtained for the two-photon centre-of-mass energies ranging in 5 GeV $\leq W_{\gamma\gamma} \leq$ 185 GeV. A steeper rise with the two-photon centre-of-mass energy as compared to the hadron-hadron and the photon-proton cross sections is observed. Several theoretical models have also been tested.

1. Introduction

At high centre-of-mass energies, $\sqrt{s}$, the two-photon process $e^+e^- \to e^+e^-$*hadrons* is a copious source of hadron production. Most of the initial energy is taken by the scattered electrons. As their scattering angle is low, they often go undetected. The hadron system has, typically, a low mass compared to $\sqrt{s}$. A large fraction of the hadrons escape detection, due to the Lorentz boost of the $\gamma\gamma$ system and to the large diffractive cross section producing hadrons at small polar angles, where the detector acceptance is limited. For these reasons, the measured visible mass, $W_{\rm vis}$, is less than the two photon effective mass, $W_{\gamma\gamma}$.

In the following, only data where the scattered electrons are not detected are considered. The statistics is based on the data collected by the L3 [1] and OPAL [2] detectors at LEP.

The two-photon cross section $\sigma(\gamma\gamma \to$ *hadrons*$)$ is derived in the interval 5 GeV $\leq W_{\gamma\gamma} \leq$ 185 GeV.

2. Event Selection

The results herein reported are based on the statistics collected by the L3 experiment at $\sqrt{s} = 130 - 202$ GeV, corresponding to and integrated luminosity of 408 pb^{-1}, and by the OPAL experiment at $\sqrt{s} = 161 - 183$ GeV, corresponding to 74 pb^{-1} of integrated

*Speaker.

luminosity. The total number of selected events amounts to 1.8×10^6 for L3 and to 0.3×10^6 for OPAL.

The selection of hadronic two-photon events is based on the central tracking system, the electromagnetic calorimeter, the hadron calorimeter and the luminosity monitor.

A typical selection of hadronic two-photon is sketched here [1]:

- to exclude scattered electrons, events with high energy clusters in the luminosity monitor are rejected. This ensures a low virtuality of the interacting photons. The distribution of low energy clusters in the luminosity monitor for L3, presented in Figure 1, shows a good agreement with both PYTHIA [3] and PHOJET[4] Monte Carlo programs.

- a moderate activity in the electromagnetic calorimeter is required, in order to suppress beam-gas and beam-wall backgrounds. It must be less than 50 GeV, to exclude radiative events, $e^+e^- \to Z\gamma$. The total energy deposited in the electromagnetic and hadronic calorimeters, $E_{\rm cal}$, must be small compared to $\sqrt{s}$, to exclude annihilation events, as shown in Figure 2.

- at least six particles must be detected, in order to exclude events containing τ.

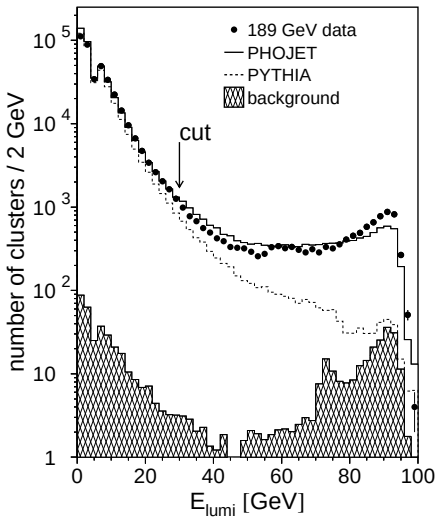

Figure 1: Energy in the luminosity monitor.

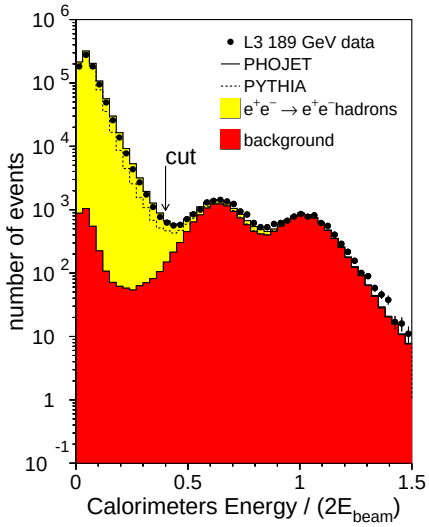

Figure 2: Energy in the electromagnetic and hadronic calorimeters, normalised to $\sqrt{s}$.

The visible effective mass of the event, $W_{\rm vis}$, is calculated from the four-momenta of the measured particles. The $W_{\rm vis}$ spectrum is shown in Figure 3 for the L3 data sample. The background is below 1% at low masses, where it is dominated by two-photon τ-pair production. It increases at high masses, due mainly to annihilation processes.

2.1 Unfolding and Cross Section Determination

The distribution of the two-photon effective mass $W_{\gamma\gamma}$ is obtained from the visible effective mass $W_{\rm vis}$ by using an unfolding procedure [5].

The result of the unfolding procedure depends on the Monte Carlo used. Data unfolded with PYTHIA are in general higher than if unfolded with PHOJET as shown in Figure 4.

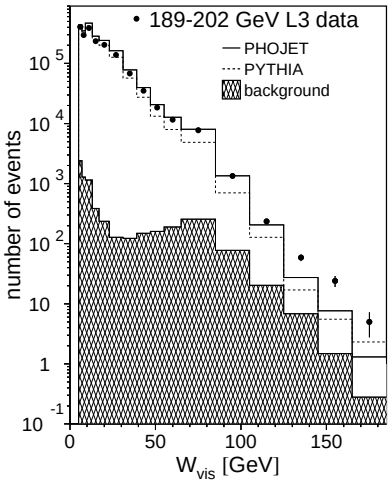

Figure 3: Distribution of the measured visible mass $W_{\rm vis}$.

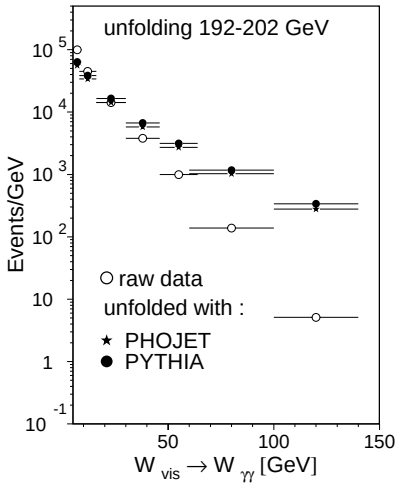

Figure 4: The measured $W_{\rm vis}$ and the resulting $W_{\gamma\gamma}$ spectrum obtained by unfolding from $W_{\rm vis}$ to $W_{\gamma\gamma}$ with PYTHIA or PHOJET Monte Carlo's.

Given the satisfactory agreement of both Monte Carlo with raw data distributions, the average of the results obtained by unfolding the data with PYTHIA and PHOJET is used. After unfolding, the events are corrected for the efficiency, using the ratio between selected and generated events in each $W_{\gamma\gamma}$ interval.

To extract the total cross section of two real photons, the luminosity function $\mathcal{L}_{\gamma\gamma}$[6] is calculated and the hadronic two-photon process is extrapolated to $Q^2 = 0$. This is done by using an analytical program [7]. The luminosity function is actually responsible for the fast decrease of the cross section as a function of $W_{\gamma\gamma}$.

The systematic uncertainties are evaluated for each $W_{\gamma\gamma}$ bin. The most important contributions come from the uncertainty on the particle multiplicity and from the Monte Carlo program used to model the process. The latter is taken as half of the difference between the results obtained by unfolding the data with PHOJET or PYTHIA and exceeds the experimental uncertainty in almost all bins.

3. Comparison with Theoretical Models

3.1 Regge Parametrisation

The total cross sections for hadron-hadron, $\sigma_{\rm pp}$, photon-hadron, $\sigma_{\gamma\rm p}$, and photon-photon, $\sigma_{\gamma\gamma}$, production of hadrons show a characteristic steep decrease in the region of low centre-of-mass energy, followed by a slow rise at high energies. From Regge theory this behavior is understood as the consequence of the exchange of Regge trajectories, $\alpha(t)$, in the t-channel. The total cross section takes the form $\sigma_{\rm tot} \propto s^{\alpha(0)-1}$. The low energy region is sensitive to the exchange of a Reggeon R ($R = \rho$, ω, f, a ..), with $\alpha_R(0) \simeq 0.5$. At high energies, the

Pomeron exchange dominates, with $\alpha_P(0) \simeq 1$. A parametrisation of the form

$$\sigma_{\rm tot} = A\, s^{\varepsilon} \,+\, B\, s^{-\eta} \tag{3.1}$$

accounts for the energy behavior of all hadronic and photoproduction total cross sections, the powers of s being universal [8]. This is confirmed by the recent compilation of the total cross section data [9] where a fit of Equation 3.1 for all hadron total cross sections gives a result compatible with the universal values $\varepsilon = 0.093 \pm 0.002$ and $\eta = 0.358 \pm 0.015$. The coefficients A and B are process and Q^2 dependent. If photons behave predominantly like hadrons, this expression may also be valid for the two-photon total hadronic cross section, with $s = W^2_{\gamma\gamma}$.

Considering only the experimental uncertainties, statistical and systematic, several Regge fits are performed on the data and their results are presented in Table 1. The exponent η is fixed to the universal value, since the low mass range is too small to be sensitive to this parameter. Using the whole $W_{\gamma\gamma}$ range, the fit with the exponents ε and η fixed to the universal value does not represent the $\sigma_{\gamma\gamma}$ energy dependence as reported in Table 1. Fits with A, B and ε as free parameters, represented as full lines in Figure 5, are performed both by L3 and OPAL. Their results are also reported in Table 1.

The fitted value of ε for L3 is more than a factor two higher than the universal value. It is independent of the Monte Carlo model used to correct the data and it is in agreement with the results obtained by the OPAL collaboration on a restricted $W_{\gamma\gamma}$ region.

	ε	χ^2/d.o.f.	CL
L3 Fixed ε	0.093	55/6	10^{-9}
L3 Free ε	0.225 ± 0.021	12/5	0.04
OPAL Free ε	0.101 ± 0.022	68/3	

Table 1: Results of the universal fit fixing or not the parameter ε.

The parameter ε is strongly correlated to the Reggeon component. To avoid this correlation, only the Pomeron exchange for sufficiently high $W_{\gamma\gamma}$ values is fitted. The value of ε increases by increasing the lower mass cutoff, thus indicating that its value is not universal, but it reflects the onset of QCD phenomena, as ε increases with increasing $W_{\gamma\gamma}$.

3.2 Models for $\gamma\gamma$ Total Cross Sections

Several models [10, 11, 12] were compared to the L3 and OPAL measurements. Their predictions for the two-photon total cross section are typically derived from measurements of proton-proton and photoproduction total cross sections via the factorization relation: $\sigma_{\gamma\gamma} \approx \sigma^2_{\gamma\rm p}/\sigma_{\rm pp}$ [13]. In general, these models give an energy dependence of the cross section similar to the universal fit discussed above. An example is shown in Figure 6 in comparison with the band constrained by γp and pp measurements.

For both lower and higher values of $W_{\gamma\gamma}$, the L3 data show a much steeper energy dependence than the theoretical predictions. Another comparison with a theoretical model and with previously measured cross sections is shown in Figure 7 [14].

In the Regge theory, the Pomeron intercept is 1, yielding a constant total cross section. When the rise of the proton-proton total cross section was first observed, it was explained

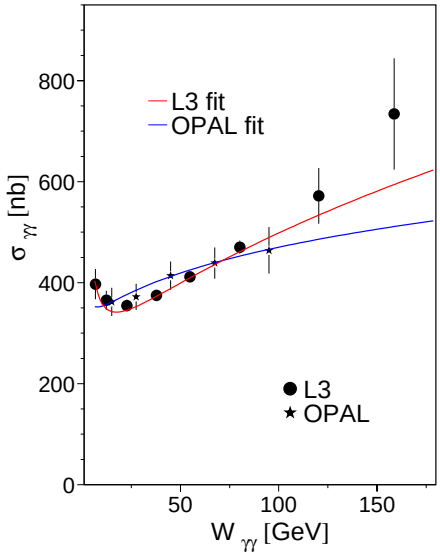

Figure 5: Two photon total cross section as measured by L3 and OPAL. Regge fits to both distributions are also shown as continuous lines.

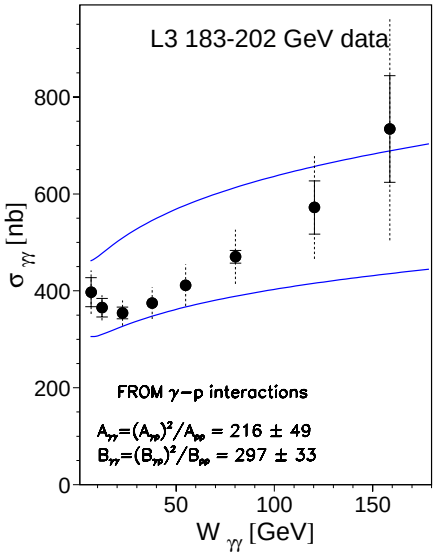

Figure 6: Measured differential cross section compared to theoretical band constrained by γp and pp measurements.

[15] with an increase of the number of hard partonic interactions. The predictions of a model [16] that calculates such effects, using an eikonalized prescription to enforce unitarity, are shown in Figure 8.

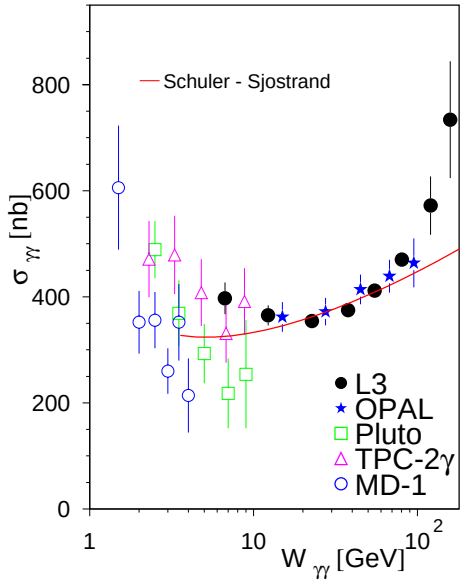

Figure 7: Predictions from Reference [14] compared to all measured differential cross section.

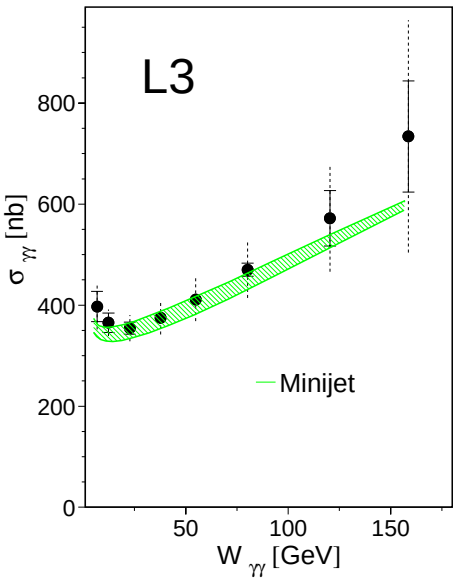

Figure 8: Predictions of the minijet model. The band correspond to different choices of the model parameters.

The parameters of the model are determined from photoproduction data and the L3 results are well inside the uncertainty related to this extrapolation.

4. Conclusions

The total $\gamma\gamma$ into hadrons cross section has been measured at LEP and compared with several theoretical models. The experimental values from L3 and OPAL experiments are in agreement between each other while on the theoretical side the models based on hard QCD processes seem to be preferred.

Acknowledgments

I would firstly thank the organizers of the conference for their warm hospitality in Budapest. The preparation of my talk and of this report would have not be possible without the help and the support of the L3-two-photon analysis group and in particular of Prof. Maria Kienzle-Focacci and Dr. Valery Andreev.
My final thanks go to the LEP machine people who have continuously overcame themselves and gave us such a good crop of data to analyse.

References

[1] L3 coll., P. Achard et al., [hep-ex/0102025].

[2] OPAL coll., K. Ackerstaff et al., *Eur. Phys. J.* **C 14** (2000) 199.

[3] T. Sjöstrand, *Comput. Phys. Commun.* **82** (1994) 74.

[4] R. Engel, *Z. Physik* **C 66** (1995) 203;
R. Engel and J. Ranft, *Phys. Rev.* **D 54** (1996) 4246.

[5] G. D'Agostini, *Nucl. Instrum. Meth.* **A362** (1995) 487.

[6] V.M. Budnev et al., *Phys. Rev.* **C 15** (1975) 181.

[7] G.A. Schuler, [hep-ph/9610406].

[8] A. Donnachie and P.V. Landshoff, *Phys. Lett.* **B 296** (1992) 227.

[9] D. E. Groom et al., *Eur. Phys. J.* **C 15** (2000) 1.

[10] G.A. Schuler and T. Sjöstrand, *Nucl. Phys.* **B 407** (1993) 539;
G.A. Schuler and T. Sjöstrand, *Z. Physik* **C 73** (1997) 67;
C. Bourrely, J. Soffer, T.T. Wu, *Mod. Phys. Lett.* **A 15** (2000) 9;
E. Gotsman et al., *Eur. Phys. J.* **C 14** (2000) 511.

[11] B. Badelek, J. Kwiecinski and A.M. Stasto, *Acta Phys. Polon.* **30** (1999) 1807;
[hep-ph/0001161].

[12] P. Desgrolard et al., *Eur. Phys. J.* **C 9** (1999) 623.

[13] V.N. Gribov and I.Ya. Pomeranchuk, *Phys. Rev. Lett.* **8** (1962) 343;
S.J. Brodsky, *J. Phys. Suppl.* (Paris) **35** (1974) C2-69.
K.V.L. Sarma and V. Singh, *Phys. Lett.* **B 101** (1981) 201.

[14] G. A. Schuler and T. Sjöstrand, *Z. Physik* **C 73** (1997) 677.

[15] D. Cline, F. Halzen and J. Luthe, *Phys. Rev. Lett.* **31** (1973) 491.

[16] R.M. Godbole and G. Pancheri, *Nucl. Phys.* **82** *(Proc. Suppl.)* (2000) 246.